THE SYNTHESIS AND LUMINESCENCE PROPERTIES OF LANTHANIDE-BASED NANOPARTICLES FOR BIOLOGICAL APPLICATION

by

MINGZHEN YAO

Presented to the Faculty of the Graduate School of

The University of Texas at Arlington in Partial Fulfillment

of the Requirements

for the Degree of

MASTER OF SCIENCE IN PHYSICS

THE UNIVERSITY OF TEXAS AT ARLINGTON

August 2008

ACKNOWLEDGEMENTS

First and foremost, I would like to express my sincere gratitude and respect to my research and thesis advisor, Prof. Dr. Wei Chen, for his invaluable guidance and constant encouragement during my research and study. His insight and expertise in nanotechnology has been my greatest source of inspiration.

I would like to thank Professors Dr. Ping Liu and Dr. Jian Yang for serving on my thesis committee. I am grateful to them for their careful and critical reading of my thesis and invaluable suggestions. Their comments and suggestions not only helped me to improve my research skills but also led me to a deeper insight into future research. I also would like to thank Dr. John L. Fry and Dr. Qiming Zhang for their invaluable suggestions, guidance, and encouragement. I am thankful to my friends and all members of our research group for their great help and friendship.

A special note of thanks goes to the McCune family, dearest friends to me and my family, for their precious friendship. Thanks to Mr. McCune for polishing my English with great patience.

Finally I would like to thank my family. I wish to express my deepest and most heartfelt gratitude to my parents for their constant encouragement and love. I am grateful to my sister and brother for their love and support. My special thanks go to my husband Tianfu Wu and son Albon Wu for always being there for me with great love and constant support. This thesis could not have been done without them.

July 9, 2008

ABSTRACT

THE SYNTHESIS AND LUMINESCENCE PROPERTIES OF LANTHANIDE-BASED NANOPARTICLES FOR BIOLOGICAL APPLICATION

MINGZHEN YAO, M.S.

The University of Texas at Arlington, 2008

Supervising Professor: WEI CHEN

Lanthanide-doped nanoparticles have great potential as a new kind of luminescent material. In this thesis, we report the synthesis of Cerium-doped LaF_3 nanoparticles in dimethyl sulfoxide (DMSO) using chemical reaction at different temperatures. We found that the emission of nanoparticles in DMSO not only depends on reaction temperature but also reaction time. The emission of DMSO solution can be tuned by reaction time, from 490 nm to 650 nm. The formation of $LaF_3:Ce^{3+}$ nanoparticles has been identified by X-ray diffraction (XRD) and transmission electron microscopy (TEM). The TEM results show that the average sizes of these nanoparticles are within 10 nm to 13 nm, which is consistent with the sizes we obtained from XRD measurement. The mechanisms for tunable emissions are being investigated. In most biological application, especially in vivo application, nanopartilces are required to be water soluble and biocompatible. Based on this concept, we have developed a simple chemical method for making high-quality, well-defined, water-soluble lanthanide-ions-doped LaF_3 nanoparticles. All the nanoparticles we synthesized are water soluble and emit very strong luminescence.

TABLE OF CONTENTS

LIST OF ILLUSTRATIONS

CHAPTER 1

INTRODUCTION

1.1 Nanotechnology

Nanotechnology is a relatively new but quickly evolving field. It is originated on December 29, 1959, when Richard Feynman, the late preeminent physicist (Nobel Prize for Physics 1965), gave a speech at the annual meeting of the American Physical Society at the California Institute of Technology. This speech, entitled “There’s Plenty of Room at the Bottom, An Invitation to Enter a New Field of Physics,” was remarkably prescient. Feynman proposed employing “machine tools to make smaller machine tools, these in turn to be used in making still smaller machine tools and so on all the way down to the atomic level.” This discussion was the earliest vision of nanotechnology.

From an strictly historical point of view, the first to mention of nanotechnology was by J. C. Maxwell, who in 1867imagined in a thought experiment a tiny entity that could manipulate individual molecules. A catalyst for the development of the modern field of nanoscience and technology was the discovery of subatomic particles, particles smaller than the atom. The work of G. J. Stoney and J. J. Thompson led to the discovery of electrons and to the development of the field of particle physics. This work led to enquiry into the nature and substance of small particles. In the 1920s, Irving Langmuir introduced the concept of a monolayer, which is a layer of material one molecule thick. Over the next half century, the development of various scanning microscopes enabled visualization and even manipulation of nano-sized structures.

Today, broadly defined, nanotechnology refers to technological study and application involving nanoparticles. The term ‘nanotechnology’ was first used by Taniguchi *et al* in 1974 [1];

they defined it as the processing, separation, consolidation, and deformation of materials by one atom or by one molecule. Drexler then popularized the field of nanotechnology by publishing two of the earliest books on the field: *Engines of Creation: The Coming Era of Nanotechnology and Nanosystems and Molecular Machinery, Manufacturing and Computation*. Later on, 'nanoscience' and 'nanotechnologies' have been defined by the Royal Society and Royal Academy of Engineering [2,3] as follows: "*Nanoscience is the study of phenomena and manipulation of materials at atomic, molecular and macromolecular scales, where the properties differ significantly from those at a larger scale*"; likewise, "*Nanotechnologies are the design, characterization, production and application of structures, devices and systems by controlling shape and size at nanometer scale*".

The term 'nanoparticle' is generally used to refer to a small particle with all three dimensions less than 100 nanometers [4]. Nanoparticles are of great scientific interest as they are effectively a bridge between bulk materials and atomic or molecular structures. A bulk material should have constant physical properties regardless of its size, but at the nano-scale this is often not the case. Size-dependent properties are observed such as quantum confinement in semiconductor particles, surface plasmon resonance in some metal particles and superparamagnetism in magnetic materials.

What is unique about nanoscale particulate matter is that, at the nanoscale level, the known physical and chemical properties of substances are altered, providing new possibilities for using the same substances only in nanosizes rather than in microsized particles. For example, the bending of bulk copper (wire, ribbon, etc.) occurs with movement of copper atoms/clusters at about the 50 nm scale. Copper nanoparticles smaller than 50 nm are considered super-hard materials that do not exhibit the same malleability and ductility as bulk copper. The change in properties is not always desirable. Ferroelectric materials smaller than 10 nm can switch their magnetization direction using room-temperature thermal energy, thus making them useless for memory storage. Suspensions of nanoparticles are possible because

the interaction of the particle surface with the solvent is strong enough to overcome differences in density, which usually result in a material either sinking or floating in a liquid. Nanoparticles often have unexpected visible properties because they are small enough to confine their electrons and produce quantum effects. For example, gold nanoparticles appear deep red to black in solution.

The main reason for this difference between nanoparticles and macroparticles of the same substance is the different surface-area-to-volume ratio, which is increased in the case of the nanoparticle. Nanoparticles have a very high surface-area-to-volume ratio. This provides a tremendous driving force for diffusion, especially at elevated temperatures. Sintering can take place at lower temperatures, over shorter time scales than for larger particles. This theoretically does not affect the density of the final product, though flow difficulties and the tendency of nanoparticles to agglomerate complicate matters. The large surface-area-to-volume ratio also reduces the incipient melting temperature of nanoparticles [5].

1.2 Applications of Nanotechnology

Recently, the use of nanotechnology has increased in many scientific disciplines, including electronics, stain-resistant clothing manufacture, and cosmetics. Nanotechnology may especially hold the promise of significant improvements in human health and well-being. Research has repeatedly shown that nanotechnology has many potential medical applications, such as in bioimaging, drug delivery, and new cancer-fighting drugs.

Molecular imaging of live cells and whole organisms is an important tool for studying cancer biology and determining the efficacy of tumor therapies. This type of visualization has been helped tremendously by the development of fluorescent probes called nanoparticles. In the fight against the pain, suffering, and death due to cancer, nanoparticles have been used in living subjects to target tissue-specific vascular biomarkers [8] and cancer cells [6, 7, 9, 10, 13]

and to identify sentinel lymph nodes in cancer [14–17]. In addition, the use of nanoparticles as fluorescent tags in cell biology [11, 13] will continue to make an impact.

Another major area of application is drug delivery. The goal is to improve contact between a drug and its target, enabling the drug to combat the disease state more efficiently. Certain characteristics of nanoparticles make them useful as carriers of active drugs. For example, their small size allows them to pass through certain biological barriers. Also, they often allow a high density of therapeutic agent to be encapsulated, dispersed, or dissolved within them. This capability depends on the preparation process, during which nanoparticles can be engineered to yield different properties and release characteristics for the entrapped agent. Because of the versatility of chemistries and preparation methods in these systems, surface functionalities can sometimes be incorporated into the nanoparticle. This facilitates additional attractive possibilities, such as the attachment of 'shielding' ligands that prolong the circulation of the nanoparticles in the blood stream, or the targeting of ligands for interaction with specific cells or tissue.

The field of nano-sized labels has generated a great deal of attention, due to their high photostability, biocompatibility, size, and composition-tunable luminescence emission from visible to near-infrared wavelengths [18-23]. Numerous articles have been devoted to more recent developments, such as plasmon resonance, surface-enhanced phenomena, metal nanoshells and semiconductor quantum dots [24-27]. In the last decade, several optical biosensors have been designed that can detect changes in the optical properties of the evanescent field of an optical surface wave, which allows the quantification of molecular recognition processes, notably antibody–antigen interactions [28-30]. So far, this field has also been extended to single-molecule detection techniques [31].

1.3 Synthesis of Nanoparticles

There are various liquid-phase methods for preparing nanoparticles, such as chemical reduction, sol-gel, reversed micelle, hot-soap, pyrolysis, and spray pyrolysis. Chemical synthesis of nanoparticles is a rapidly growing field with great potential for making useful materials [32]. Chemical synthesis permits the manipulation of matter at the molecular level. Because of mixing at the molecular level, good chemical homogeneity can be achieved. Also, by understanding the relationship between how matter is assembled on an atomic and molecular level and the material's macroscopic properties, molecular synthetic chemistry can be designed to prepare novel starting components. Better control of particle size, shape, and size distribution can be achieved in particle synthesis.

1.3.1 Nucleation and Growth from Solutions

Precipitation of a solid from a solution is a common technique for the synthesis of fine particles. The general procedure involves reactions in aqueous or non-aqueous solutions containing the soluble or suspended salts. Once the solution becomes supersaturated with the product, a precipitate is formed by either homogeneous or heterogeneous nucleation. Homogeneous and heterogeneous nucleation refers to the formation of stable nuclei with or without foreign species respectively. After the nuclei are formed, their growth usually proceeds by diffusion. In diffusion-controlled growth, concentration gradients and temperature are important in determining the growth rate. To form mono-dispersed particles, i.e. unagglomerated particles with a very narrow size distribution, all the nuclei must form at nearly the same time, and subsequent growth must occur without further nucleation [33] or agglomeration of the particles.

In general, particle size and particle-size distribution, amount of crystallinity, crystal structure, and degree of dispersion can be affected by reaction kinetics. Factors influencing the rate of reactions include the concentration of reactants, reaction temperature, pH, and the order

in which the reagents are added to the solution. A multi-element material is often made by co-precipitation of the batched ions. However, it is not always easy to simultaneously co-precipitate all the desired ions, since different species may precipitate at different pH levels. Thus, special attention is required to control chemical homogeneity and stoichiometry. Phase separation may be avoided during liquid precipitation and homogeneity at the molecular level improved by converting the precursor to powder form by using spray drying [34] or freeze drying [35].

1.3.2 Stabilization of Fine Particles against Agglomeration

Fine particles, particularly nanoscale particles, since they have large surface areas, often agglomerate to form either lumps or secondary particles, thus minimizing the total surface or interfacial energy of the system. When the particles are strongly stuck together, these hard agglomerates are called *aggregates*. Many materials containing fine particles, some examples of which include paints, pigments, electronic inks, and ferrofluids, are useful if the particles in the fluid suspension remain unagglomerated or dispersed. Agglomeration of fine particles can occur at the synthesis stage or during drying and subsequent processing of the particles. Thus it is very important to stabilize the particles against adverse agglomeration at each step of particle production and powder processing. Surfactants are used to produce dispersed particles in the synthesis process or to disperse synthesized agglomerated fine particles.

Many technologies use surfactants [36, 37]. A surfactant is a surface-active agent that has an amphipathic structure in that solvent, i.e. a lyophobic (solvent repulsive) and lyophilic group (solvent attractive). Depending on the charges at the surface-active portions, surfactants are classified as either anionic, cationic, zwitterionic (bearing both positive and negative charges), or non-ionic (no charges). At low concentrations, the surfactant molecules absorb on the surfaces or interfaces in the system, and can significantly alter the interfacial energies.

Agglomeration of fine particles is caused by the attractive van der Waals force and/or the driving force that tends to minimize the total surface energy of the system. Repulsive

interparticle forces are required to prevent the agglomeration of these particles. Two methods are commonly used. The first stabilization method causes dispersion using electrostatic repulsion. Repulsion results from the interactions between a particle's surface and the solvent. Electrostatic stabilization of a dispersion occurs when the electrostatic repulsive force overcomes the attractive van der Waals forces between particles. This stabilization method is generally effective in dilute systems of aqueous or polar organic media. It is very sensitive to the electrolyte concentration, since a change in concentration may destroy the electric double layer, resulting in particle agglomeration.

The second stabilization method involves the use of steric forces. Surfactant molecules can adsorb onto the surfaces of particles and their lyophilic chains will then extend into the solvent and interact with each other. The solvent chain interaction, which is a mixing effect, increases the free energy of the system and produces an energy barrier to the closer approach of particles. When particles come into closer contact with each other, the motion of the chains extending into the solvent is restricted, producing an effective barrier in both aqueous and non-aqueous media, one less sensitive to impurities or trace additives than when using electric stabilization. The steric stabilization method is particularly effective in dispersing high concentrations of particles.

1.4 Structural Characterization of Nanoparticles

Nanoparticle characterization is necessary for establishing understanding and control of nanoparticle synthesis and applications. Characterization uses a variety of different techniques, mainly drawn from materials science. Common techniques are electron microscopy [TEM,SEM], atomic force microscopy [AFM], dynamic light scattering [DLS], x-ray photoelectron spectroscopy [XPS], powder x-ray diffractometry [XRD], Fourier transform infrared spectroscopy [FTIR], Matrix-Assisted Laser-Desorption Time-of-flight mass spectrometry [MALDI-TOF], and ultraviolet-visible spectroscopy.

X-ray diffraction is the preferred method for examining the formation of the crystalline assembly, provided the sample size is sufficient. The diffraction spectrum at the high-angle range is directly related to the atomic structure of the nanoparticles, whereas the spectrum at the lower angle region is directly associated to the ordered assembly of nanocrystals [38, 39]. By examining the diffraction peaks that are extinct in the spectrum, one may identify the crystallography of the packing. This analysis is based on the assumption that each particle is identical in size, shape, and even orientation, so that the extinction rules derived from diffraction physics apply.

Scanning electron microscopy (SEM) is a powerful technique for imaging the surfaces of almost any material. It is likely the most popular tool for material characterization. A modern SEM can furnish a resolution of 1 nm, relatively simple image interpretation, and large depth of focus, making it possible to directly image the 3D structure of nanomaterials. Transmission electron microscopy (TEM), as a high spatial resolution structure and chemical microanalysis tool, has been proven to be powerful for characterization of nanomaterials [40]. A modern transmission electron microscope can directly image atoms in crystalline specimens at resolutions close to 0.1 nm, smaller than interatomic distance. An electron beam can also be focused to a diameter smaller than 0.3 nm, allowing quantitative chemical analysis from a single nanocrystal. This type of analysis is extremely important for characterizing materials at a length scale from atoms to hundreds of nanometers. Determining the shape of nanocrystals is an important application of TEM. Using a combination of high-resolution lattice imaging and possibly electron diffraction, the crystal structure and facets can be determined.

Photoluminescence spectroscopy is a contactless, nondestructive method of probing the electronic structure of materials. Light is directed onto a sample, where it is absorbed and imparts excess energy into the material in a process called photo-excitation. One way this excess energy can be dissipated by the sample is through the emission of light, or luminescence. In the case of photo-excitation, this luminescence is called photoluminescence.

The intensity and spectral content of this photoluminescence is a direct measure of various important material properties. Photo-excitation causes electrons within the material to move into permissible excited states. When these electrons return to their equilibrium states, the excess energy is released and may include the emission of light (a radiative process) or may not (a nonradiative process). The energy of the emitted light (photoluminescence) relates to the difference in energy levels between the two electron states involved in the transition between the excited state and the equilibrium state. The quantity of the emitted light is related to the relative contribution of the radiative process.

Shape, size and ambient conditions are crucial parameters in understanding the physics and chemistry phenomena of matter at the nanometer scale. The promising technological applications of nanoscience depend on our capacity to control these parameters. In particular, a correct understanding of the optical properties of nanostructures is essential. Optical techniques, such as Raman, differential and anisotropy reflectance spectroscopy, light absorption spectroscopy, surface enhanced Raman scattering (SERS), etc., can be powerful tools for characterizing nanostructures because of their non-destructive and real-time character, together with their *in situ* potentiality. Furthermore, optical spectroscopies provide statistical properties of the whole sample. These attributes have allowed us to control the growth of superlattices [41], and the growth of nanoparticles, correcting their shape and size during the process. Optical spectroscopies can also be used as complementary tools of the structural characterization techniques such as atomic force microscopy (AFM), scanning tunneling microscopy (STM), transmission electron microscopy (TEM), etc., which provide the image of a small piece of the sample, giving information about local properties and characterizing a few nanoparticles at a time.

1.5 Lanthanide-Based Nanoparticles

Lanthanide-based nanoparticles have shown great potential for use as luminescent materials. The successful use of highly luminescent rare-earth doped nanoparticles, combining the various properties of doping ions and the nanoparticle matrix, have ensured the expanded use of nanoparticles. Multifunctional nanoparticles can be tailored for detecting or tracking labeled biomolecules with several complementary techniques [42], for facilitating the separation and detection of biomolecules [43], or for performing both diagnosis and therapy [44]. Replacement of organic dyes with inorganic fluorophores, such as lanthanide compounds (Yb, Er) [45], is an interesting strategy for synthesizing efficient luminescent multifunctional nanoprobes, because the lanthanide ions exhibit advantageous optical properties. As they are characterized by high photostability, a long luminescence lifetime (1 ms), narrow emission bands, and a broad absorption band, lanthanide ions are indeed very well suited for elaboration of highly luminescent and photostable nanoprobes [46] without emission intermittency. Kennedy *et al* demonstrated that Eu_2O_3 nanoparticles can be applied as a fluorescent label in an immunoassay for atrazine with good sensitivity [47]. Biolabeling can also be performed with Eu^{3+} chelates dispersed in silica particles [48]. Moreover, a large palette of colors can be easily obtained by a convenient choice of lanthanide ions [46]. In contrast to quantum dot, the color of the emitted light does not depend on the size of the fluorescent nanoparticles, but only on the nature of the lanthanide ions, therefore avoiding formation of motley particles and a cumbersome purification step. LaF_3 was chosen as the host matrix because this material has very low vibrational energies [49], thus minimizing the quenching of the excited state of the rare earth ions. This is especially important for the rare-earth ions emitting in the near-infrared part of the spectrum, because they are very sensitive to quenching by high-energy vibrations [50]. Despite their numerous advantages, development of highly luminescent lanthanide-ion-doped nanoparticles was impeded by the lack of efficient synthetic routes. In this study, we report the synthesis of lanthanide fluoride nanoparticles doped with cerium in organic solvent (DMSO) in

Chapter 2, water-soluble lanthanide fluoride nanoparticles doped with Ln^{3+} ions (Ln = Ce^{3+}, Tb^{3+}, Ce^{3+} and Tb^{3+}) in Chapter 3. Furthermore, we discuss structural characterization as well as luminescent properties -- these nanoparticles all display strong luminescence.

CHAPTER 2

LUMINESCENCE PROPERTIES OF CE^{3+} DOPED LAF_3 NANOPARTICLES IN DMSO

2.1 Introduction

Lanthanide-based nanocrystals have shown great potential for use as luminescent materials due to electronic transitions within the 4f shell of the trivalent lanthanide ions [51, 52]. In particular, a very large interest in using Lanthanide-based nanoparticles (NPs) has developed due to their higher photo stability and luminescence compared to organic dyes [53]. As a result, they are becoming highly favored for biological applications such as bioconjugation due to their physical and optical properties [54].

The synthesis process and spectroscopic properties of Lanthanide (III)-doped nanoparticles have attracted more considerable interest since they are used in biological applications [55,56]. LaF_3 is an ideal material for various phosphors because this material has very low phonon energy and thus the quenching of the excited state of the lanthanide ions will be minimal. Of the many routes taken to impart biological activity to NP, bioconjugation of proteins to luminescent particles stabilized with ethylene glycol [H(OCH2CH2)nOH, PEG] is among the most common. The biological advantage of covalently attaching NPs to biological macromolecules, such as peptided and proteins, with PEG chains (commonly referred to as PEGylation) is that it allows for suppression of antigenic and immunogenic epitopes, and prevents recognition and degradation by proteolytic enzymes [47,58]. Furthermore, the hydrophilic nature of PEG is an excellent ligand to render these NPs water soluble. Here, we report the development of LaF_3-based NPs that are doped with Ce^{3+} in Dimethyl Sulfoxide (DMSO) with PEG as stabilizer. The use of DMSO (Dimethyl Sulfoxide) as a pharmaceutical has been surrounded with all kinds of controversies since 1961 [59]. Recently, people have

found out that DMSO has many useful applications. Especially some researchers have proved that DMSO can carry other drugs with it across membranes [60]. It is more successful ferrying some drugs, such as morphine sulfate, penicillin, steroids, and cortisone, than others, such as insulin. What it will carry depends on the molecular weight, shape, and electrochemistry of the molecules. This property would enable DMSO to act as a new drug delivery system that would lower the risk of infection occurring whenever skin is penetrated. By using DMSO as solvent, we synthesized $LaF_3:Ce^{3+}$ nanoparticles with special emissions.

2.2 Experimental Section

2.2.1 Nanoparticle Synthesis

Lanthanum (III) nitrate hydrate ($La(NO_3)_3 \cdot XH_2O$, 99.9%), Cerium (III) nitrate hexahydrate ($Ce(NO_3)_3$ $6H_2O$,99.9%), ammonium fluoride (NH_4F, 99.9%), poly(ethylene glycol) bis(carboxymethyl) ether were purchased from Sigma-Aldrich. All of the reagents were used as received, without further purification. $LaF_3:Ce^{3+}$ Nanoparticles were synthesized by wet-chemistry method. Typically, 9 mmol of $La(NO_3)_3$, 1 mmol of $Ce(NO_3)_3$ and 30 mmol of NH_4F were added into 50 ml dimethyl sulfoxide (DMSO) in a three-necked flask, 1ml PEG was added to the mixture as stabilizer to prevent the particles from aggregation. In this work, $Ce(NO_3)_3$ were used as dopant at the concentration of 0.1 M. The chemicals were mixed thoroughly with stirring for half and hour at room temperature, the mixture was subsequently heated to three different temperatures -- 70° C, 150° C and 180° C respectively, under vigorous magnetic stirring and nitrogen protection. A suspension formed gradually upon stirring. The color of the samples under high temperatures (150° C and 170° C) changed from white to yellow, however, the one of under low temperature (70° C) changed a little bit from white to light yellow. The nanocrystals obtained were collected by centrifugation, washed with DI water and 0.5% acetic acid solution several times, and stored in DI water.

2.2.2 Characterization

The $LaF_3:Ce^{3+}$ nanoparticles were characterized with high resolution Transmission electron microscopy (TEM) images were taken using a JEOL JEM-2100 instrument, with accelerating voltage of 200 kV. Samples for TEM were prepared by depositing a drop of a colloidal aqueous solution of the powder sample onto a carbon-coated copper grid. The excess liquid was wiped away with filter paper, and the grid was dried in air. The X-ray powder diffraction (XRD) patterns of LaF3:Ce3+ nanoparticles were recorded in the range of $20^{\circ} \leq 2\theta \leq 80^{\circ}$ from Siemens Kristalloflex 810 D-500 X-ray diffractometer under operating mode of 40 kV and 30 mA with λ=1.5406 Angstrom radiation. The emission and excitation spectra of the samples were measured by using a Shimadzu fluorescence spectrometer (RF-5301PC) with a 400W monochromatized xenon lamp.

2.3 Results and Discussion

2.3.1 XRD Pattern and TEM Characterization of the $LaF_3:Ce^{3+}$ Nanoparticles

Figures 2.1 and 2.2 show the XRD patterns of the $LaF_3:Ce^{3+}$ nanoparticles synthesized at two different high temperatures. The peak positions and intensities are consistent with the data reported in the JCPDS standard card (32-0483) of pure hexagonal Lanthanum Fluoride crystals. However, the 113 peak is decreased its sharpness when the temperature is increased. The sizes of the nanocrystals were calculated from the XRD pattern based on the Debye–Scherrer formula, assuming that all the particles are spherical in shape. The average size of nanoparticles produced at 180º C is about 8 nm, and the one of that produced at 150º C is about 10nm.

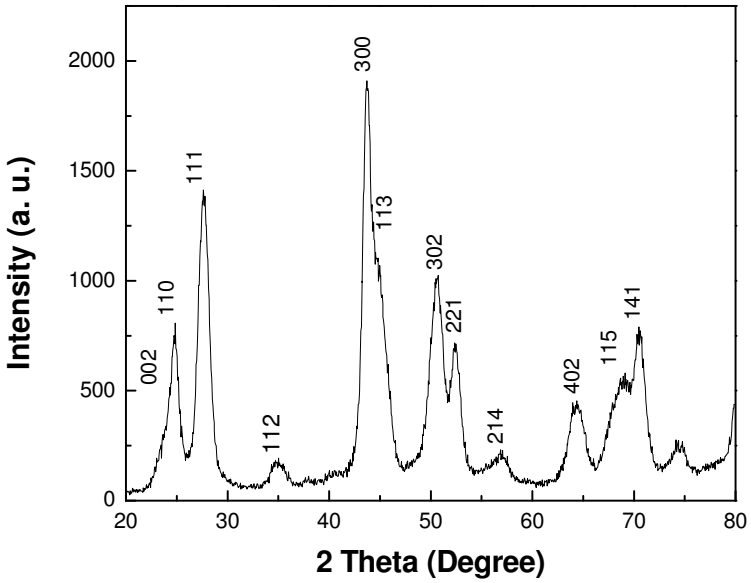

Figure 2.1 XRD pattern of $LaF_3:Ce^{3+}$ nanoparticles synthesized at 180ºC

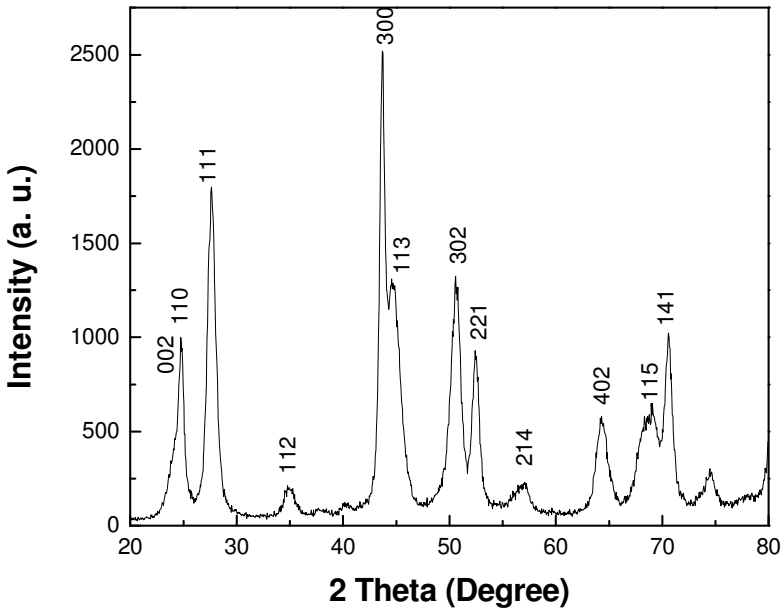

Figure 2.2 XRD pattern of $LaF_3:Ce^{3+}$ nanoparticles synthesized at 150ºC

Figure 2.3 shows high resolution TEM images of the $LaF_3:Ce^{3+}$ nanocrystals synthesized under high temperature. It can be seen that the nanocrystals are well dispersed in solution, the shape of the $LaF_3:Ce^{3+}$ nanoparticles is spherical and the average diameter is around 10-15 nm, which is consistent with the size obtained by XRD measurement. The HRTEM images of $LaF_3:Ce^{3+}$ nanoparticles indicate that $LaF_3:Ce^{3+}$ have high crystalline quality as evidenced by the clear lattice fringes in the inset image. Figure 2.4 shows the high resolution TEM images of $LaF_3:Ce^{3+}$ nanocrystals synthesized under low temperature. It can be seen that the nanoparticles have a certain degree of aggregation, but for the single nanoparticles, each of them has spherical shape with average size of 8 nm. In all, the HRTEM images of LaF_3: Ce nanoparticles shown in Figures 2.3 and 2.4 indicate that all the particles have high crystalline quality. The fringes are from the [200] planes and the atomic plane distance measured is about 3.13 Á which is very close to the plane distance (3.112 Á) measured by X-ray diffraction [61]. The fringes are from the [121] and [211] planes and the atomic plane distance measured is about 3.33 Á which is very close to the plane distance (3.23 Á) reported by Yanes *et al* [62].

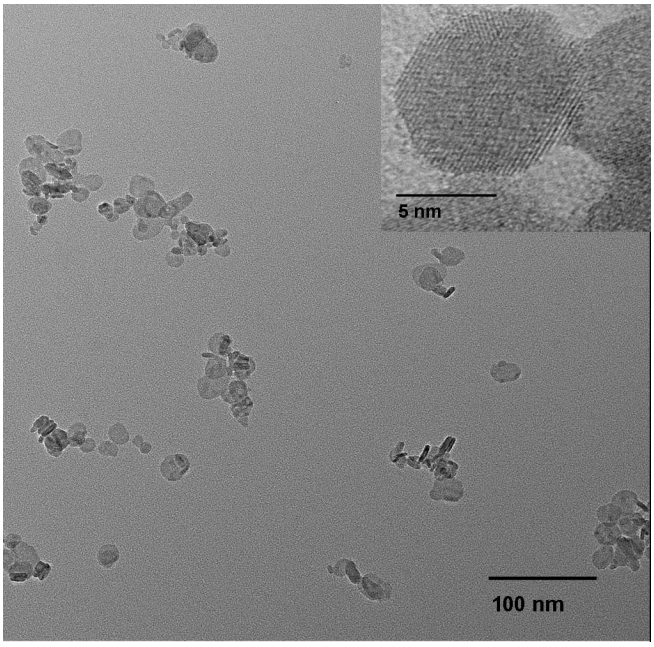

Figure 2.3 HRTEM images of $LaF_3:Ce^{3+}$ nanoparticles synthesized at 150ºC

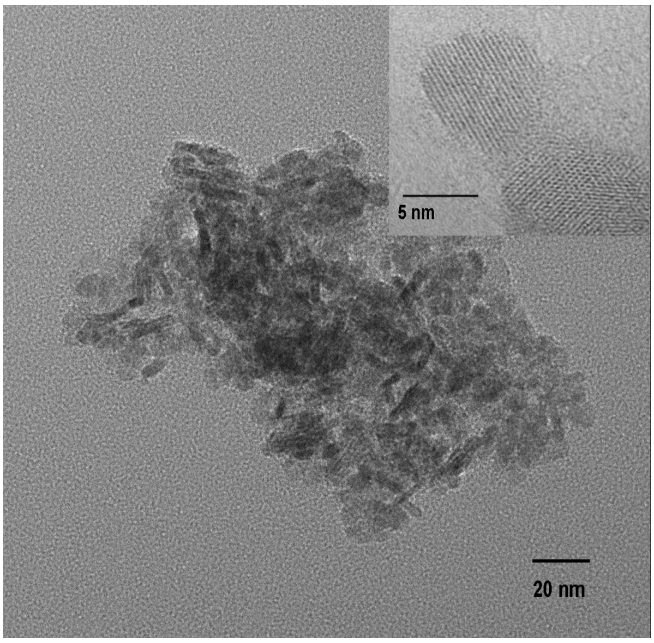

Figure 2.4 HRTEM images of $LaF_3:Ce^{3+}$ nanoparticles synthesized at 70ºC

2.3.2 Luminescence Property

In Figure 2.5, excitation and emission spectra of samples at two high temperatures (180º C and 150º C) and a low temperature (70º C) were compared upon excitation at 255 nm. All three samples have the same emission around 311 nm, which is related to the 5d-4f transitions of the Ce ion [63, 64]. Figure 2.6 shows excitation and emission spectra of $LaF_3:Ce^{3+}$ under 180º C and 150º C in the long wavelength area. Compared to the emission of the sample at 468nm under 150º C, emission of the sample under 180º C shifts to the longer wavelength around 497nm. It should be noted that although the emissions in the long wavelength area are also observed in the sample under 70º C, here they are in the shorter wavelength region, between 375nm and 421nm (see Figures 2.7 and 2.8). We conclude that the emission of the long wavelength in the sample depends heavily on the reaction temperature. The higher the reaction temperature, the longer the wavelength emission.

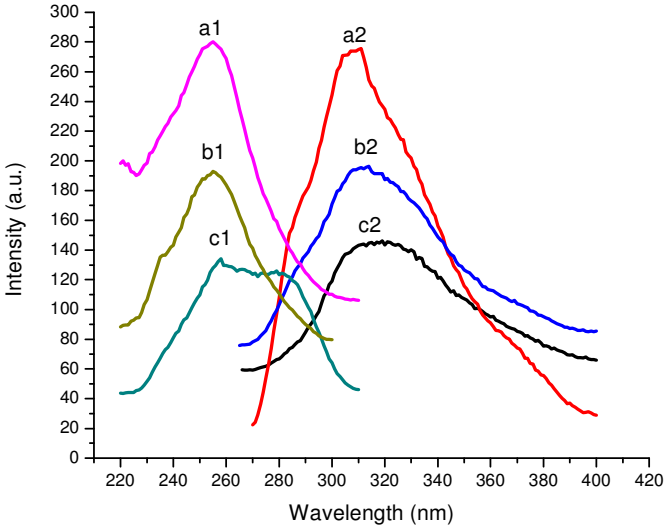

Figure 2.5 Excitation and Emission spectra of three samples under different temperatures: a1 and a2 is the excitation and emission spectrum for sample under 150º C (emission at 306 nm, excited at 255 nm); b1 and b2 are the excitation and emission spectrum for sample under 180º C (emission at 311 nm, excited at 255 nm); c1 and c2 are the excitation and emission spectrum for sample under 70º C (emission at 320 nm, excited at 255 nm).

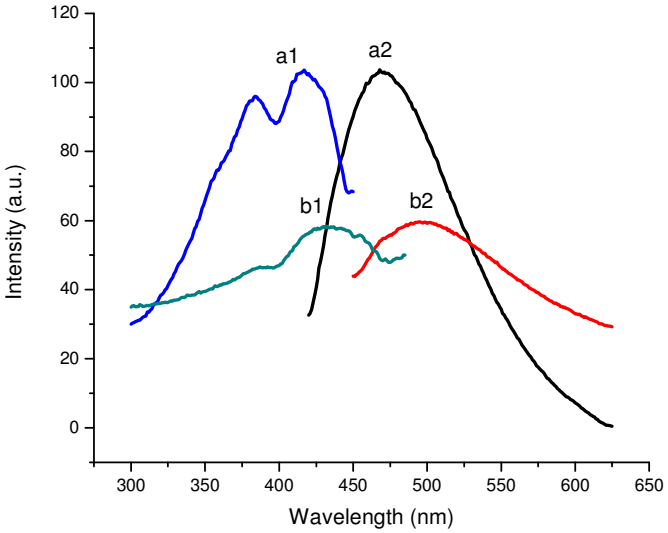

Figure 2.6 Excitation and emission spectra of two high-temperature samples: a1 and a2 is the excitation and emission spectrum for sample under 150º C (emission at 468 nm, excited at 400 nm); b1 and b2 are the excitation and emission spectrum for sample under 180º C (emission at 497 nm, excited at 430 nm).

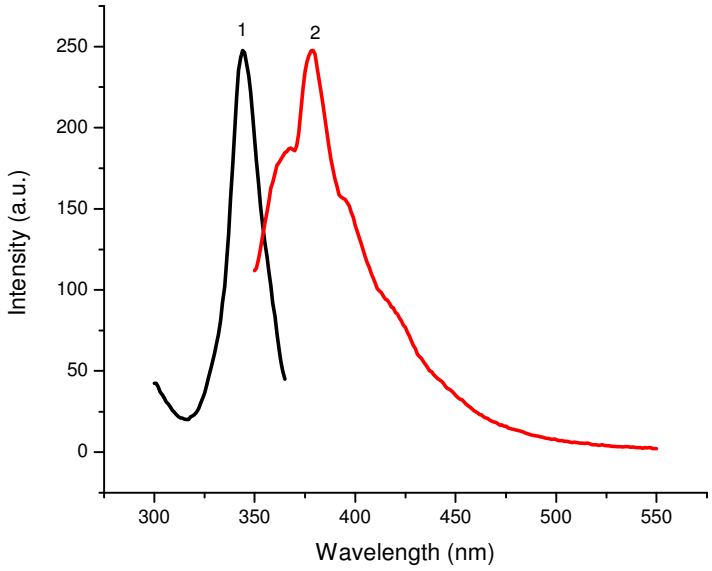

Figure 2.7 Fluorescence emissions of $LaF_3:Ce^{3+}$ at low temperature (70º C) reaction time 2.5 hrs: 1-- Excitation spectrum (emission at 375 nm); 2 -- Emission spectrum (excited at 340 nm)

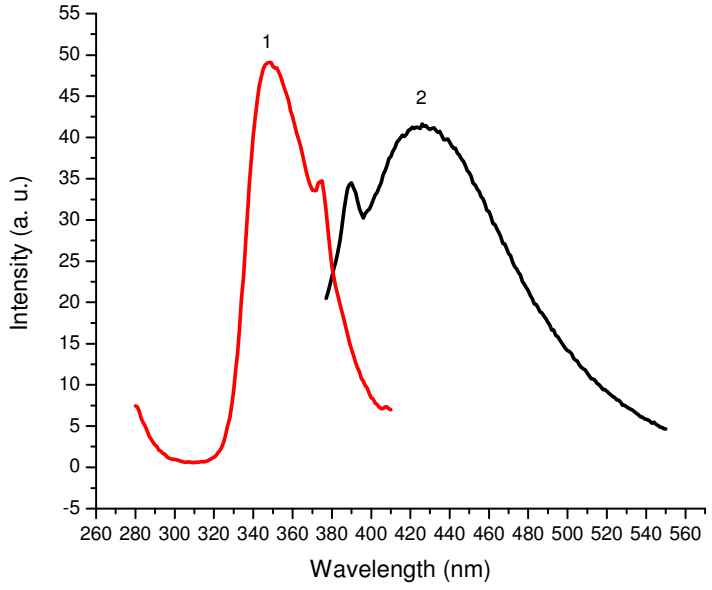

Figure 2.8 Fluorescence emissions of $LaF_3:Ce^{3+}$ at low temperature (70º C) reaction time 4.5 hrs: 1-- Excitation spectrum (emission at 421 nm); 2-- Emission spectrum (excited at 350 nm)

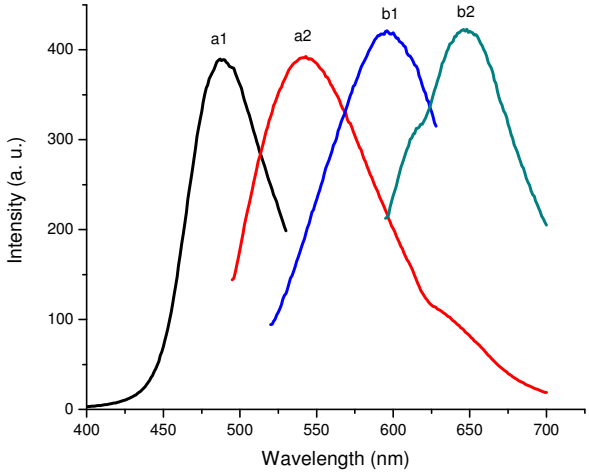

Figure 2.9 Excitation and emission spectrum of two high-temperature samples in solution: a1 and a2 is the excitation and emission spectrum for sample under150º C (emission at 543 nm, excited at 487 nm); b1 and b2 are the excitation and emission spectrum for sample under 180º C (emission at 648 nm, excited at 587 nm).

Figure 2.9 shows the emission spectra of the samples measured in DMSO solution. Interestingly, even longer wavelength luminescence in the solution can be observed around 600 nm. Again compared to the emission of sample at 150º C, the emission of the sample at 180º C shifts to the longer wavelength. To find out if emissions of $LaF_3:Ce^{3+}$ nanoparticles in DMSO depend on reaction time, we investigate the luminescence properties of the samples at different reaction time shown in Figure 2.10. These emission spectra of samples in solution were measured at room temperature, both with slit widths of 3 nm. The figure shows that emission intensity of the sample increases greatly when reaction time is prolonged to 1.5 hrs. Overall, emission shifts to long wavelength from 490 nm to 650 nm according to the reaction time. These emissions are probably induced by the corresponding metal complex which could be formed as part of intermediate products during the chemical reaction. The details need to be further investigated. This phenomenon shows that fluorescence of the $LaF_3:Ce^{3+}$ nanoparticles were remarkably influenced by reaction time and reaction temperature. Optimal reaction

temperature of 3 hrs was concluded from these systematic experiments. In addition, it was found that the higher the temperature, the longer the nanoparticles' wavelength emission.

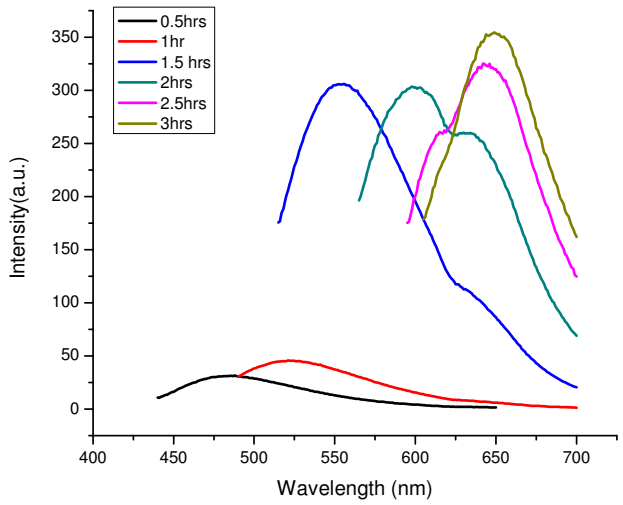

Figure 2.10 Fluorescence emissions of $LaF_3:Ce^{3+}$ at different reaction time under high temperature

To find out the luminescence mechanism of $LaF_3:Ce^{3+}$ nanoparticles in DMSO, we use the same chemical $Ce(NO_3)_3$ $6H_2O$ (99.9%) as the one we use for synthesis of $LaF_3:Ce^{3+}$ nanoparticles in DMSO, with the same concentration, same reaction temperature, same reaction time. Figure 2.11 shows the luminescence comparison of Ce+DMSO and $LaF_3:Ce^{3+}$ in DMSO under 180º C. The emission from Ce+DMSO is consistent with the emission of $LaF_3:Ce^{3+}$ powder nanoparticles under 180º C. The emission peak from LaF3:Ce solution is still unknown. In order to test this phenomenon, we use the same method to investigate the luminescence properties of Ce+DMSO and La+DMSO, then compare them with $LaF_3:Ce^{3+}$ nanoparticles in DMSO under 150º C. Figure 2.12 shows the comparison of emission peaks. Again, the emission from Ce+DMSO is completely consistent with the emission of $LaF_3:Ce^{3+}$ powder nanoparticles under 150º C. The emission of La+DMSO is about 630 nm, which is far different from the emission from LaF3:Ce solution. Therefore, we conclude that the powder nanoparticles we obtained contain two configurations: one is $LaF_3:Ce^{3+}$ nanoparticles, the other

is Ce+DMSO complex. Comparing emission intensity of samples at 311 nm and at long wavelength in Figure 2.5 and Figure 2.6, we infer the main product we obtained is $LaF_3:Ce^{3+}$ nanoparticles.

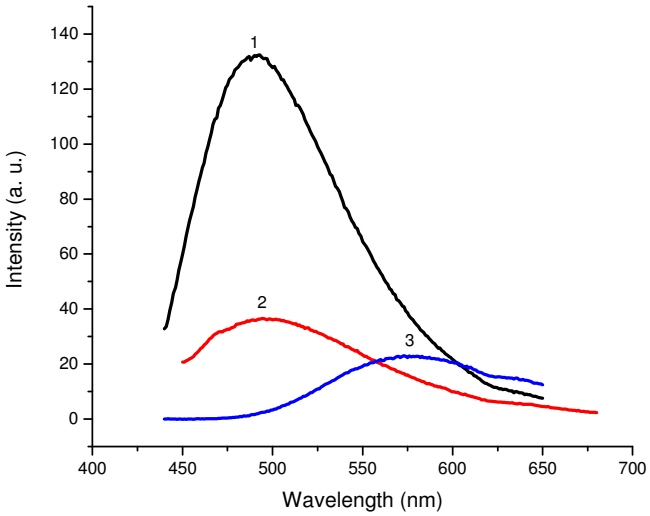

Figure 2.11 Comparison of emission spectra excited at 430 nm:
Ce in DMSO; 2 -- LaF3: Ce Powder (180º C); 3 -- LaF3:Ce solution (180º C)

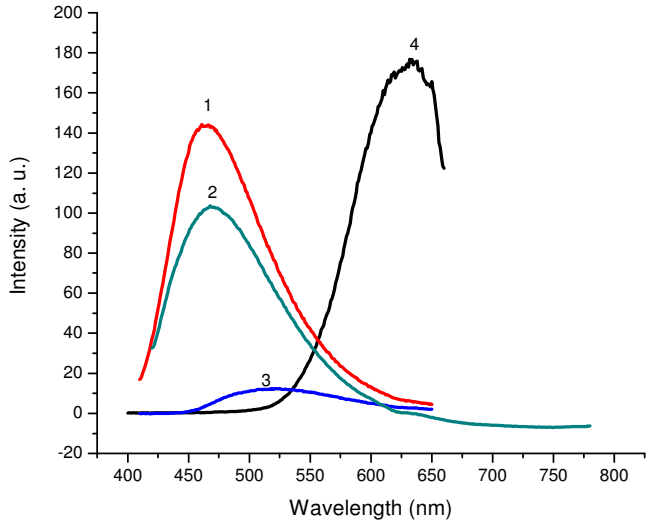

Figure 2.12 Comparison of emission spectra excited at 400 nm:
Ce in DMSO; 2 -- LaF_3: Ce powder (150º C); 3 -- LaF^3:Ce solution(150º C); 4 -- La in DMSO

2.4 Conclusion

Lanthanide-based nanoparticles have shown great potential for use as luminescent material. In this chapter, we report the synthesis of LaF_3 doped with cerium in dimethyl sulfoxide (DMSO) and investigate the luminescence property of this type of nanoparticle. Cerium-doped LaF_3 have been prepared in a thermal process in DMSO at different temperature and different reaction period. The samples under either low temperature or high temperature have the same emission peak at 311 nm, which are related to the 5d→4f transitions of the Ce ion. Another peak is in the 450-650 nm region. Compared to the emission of the sample under 150º C, emission of the sample under 180º C shifts to the longer wavelength around 497 nm. However, the emission in the sample under 70º C is observed to be around 400 nm. Also, the emission of the sample is greatly dependent on the reaction time; it can be tuned by time from 490-650 nm for high-temperature samples. The X-ray diffraction (XRD) pattern shows that LaF_3:Ce was produced in high-temperature samples. From the emission spectra, besides $LaF_3:Ce^{3+}$ nanoparticles, we find that Ce+DMSO complex might have been formed in the samples under high temperature. Transmission electron microscopy (TEM) shows the average sizes of these nanoparticles ranging from 10 nm to 13 nm. Since the properties of DMSO enable it to act in new drug delivery, the $LaF_3:Ce^{3+}$ nanoparticles produced in DMSO solution could be better used in biological applications. The use of tunable emissions for this material holds great promise for biological fluorescent labels and cancer detection.

CHAPTER 3

LUMINESCENCE PROPERTIES OF LN^{3+} DOPED LAF_3 NANOPARTICLES IN WATER

3.1 Introduction

Fluorescent labeling of molecules is a common and very useful technique in biological science. LnF_3-based nanoparticles could have a number of advantages for use as probes in bioconjugation applications over other biolabels, since emissions from lanthanide ions involve f-orbital electrons and are much narrower than those observed from organic molecules. The quantum yield of lanthanide emission is high in the absence of quenching and photobleaching effects which are commonly observed in fluorescent dye molecules, but not observed in lanthanide ions. In addition, LnF_3-based nanoparticles have a number of advantages as probes used in bioconjugation applications over other biolabels, such as inherent long-lived luminescent lifetimes and long-term stability of the nanoparticle signal. In recent years, some research in this area confirmed that Ln^{3+} doped LnF_3 can be turned into biolabels with some specific binding to proteins [65-67]. Different methods have been used to synthesize LnF_3-based nanoparticles [68-74]. However, most LnF_3 nanoparticles that are synthesized so far are not water soluble or biocompatible, which greatly limits their application in biological systems. Here we report the synthesis of LaF_3: Ce nanopowder and Ln^{3+} doped LaF_3 nanoparticles (Ln^{3+} refers to Tb^{3+}, Tb^{3+}+Yb^{3+} and Tb^{3+}+Ce^3 which are water soluble directly without need of additional coating work. The investigation of luminescent properties is detailed in Sections 3.2 and 3.3 respectively.

3.2 Synthesis and Luminescence Property of LaF3:Ce^{3+} Nanopowder

3.2.1 Synthesis of LaF3:Ce^{3+} Nanopowder

Lanthanum (III) nitrate hydrate ($La(NO_3)_3 \cdot X\ H_2O$, 99.9%), Cerium (III) nitrate hexahydrate ($Ce(NO_3)_3\ 6H_2O$,99.9%), ammonium fluoride (NH_4F, 99.9%), poly(ethylene glycol) bis(carboxymethyl) ether were purchased from Sigma-Aldrich. All reagents were used directly, without further purification. LaF_3:Ce^{3+} nanoparticles were synthesized using the wet-chemistry method. Typically, 9 mmol of $La(NO_3)_3$, 1 mmol of $Ce(NO_3)_3$ and 30 mmol of NH_4F were added to 50 ml water in a three-necked flask, 1 ml of PEG was added dropwise to the mixed chemical solution. A PEG-based backbone for ligand 1·(2NH4+) was used because PEG is known to be a hydrophilic ligand, which allows for the NP to be synthesized and analyzed under aqueous conditions. In this work, $Ce(NO_3)_3$ was used as dopant at the concentration of 0.1 M. The chemicals were mixed thoroughly with stirring for half an hour at room temperature; the mixture was subsequently heated to 100° C under vigorous magnetic stirring and nitrogen protection. A white suspension was formed gradually upon stirring. The nanoparticles obtained were collected by centrifugation, washed with DI water several times, then stored in DI water.

3.2.2 Characterization of LaF3:Ce^{3+} nanopowder

The LaF_3:Ce^{3+} nanoparticles were characterized with high-resolution transmission electron microscopy (TEM). Images were taken with a JEOL JEM-2100 instrument, with accelerating voltage of 200 kV. Samples for TEM were prepared by depositing a drop of a colloidal aqueous solution of the powder sample onto a carbon-coated copper grid. The excess liquid was wiped away with filter paper, and the grid was dried in air. The X-ray powder diffraction (XRD) patterns of LaF3:Ce3+ nanoparticles were recorded in the range of 20◦ ≤2θ ≤80° from a Siemens Kristalloflex 810 D-500 X-ray diffractometer under an operating mode of 40 kV and 30 mA with λ=1.5406 Angstrom radiation. The emission and excitation spectra of the samples were

measured using a Shimadzu fluorescence spectrometer (RF-5301PC) with a 400W monochromatized xenon lamp.

Figure 3.1 shows the XRD patterns of the $LaF_3:Ce^{3+}$ nanoparticles synthesized in water. The peak positions and intensities are consistent with the data reported in the JCPDS standard card (32-0483) of pure hexagonal Lanthanum Fluoride crystals. The sizes of the nanocrystals were calculated from the XRD pattern based on the Debye–Scherrer formula, assuming that all the particles are spherical in shape. The results show that the size of the nanoparticles produced is about 16nm.

Figures 3.2 and 3.3 show the high-resolution TEM images of the $LaF_3:Ce^{3+}$ nanocrystals. It can be seen in Figure 3.2, with 40K magnification, that the nanocrystals are well dispersed and the shape of the $LaF_3:Ce^{3+}$ nanoparticles are spherical. Figure 3.3 shows an 800K-magnified TEM image of $LaF_3:Ce^{3+}$ nanocrystals, in which clear lattice fringes are evidence of crystalline quality. The size of the nanoparticles is about 15 nm, which is consistent with the size obtained from XRD measurement.

Figure 3.4 shows the excitation and emission spectra of $LaF_3:Ce^{3+}$ nanocrystals at different reaction time from 1 hour to 11 hours. These samples all have the same emission peak at 343 nm, which was attributed to the 5d-4f transitions of the Ce ion. The intensity of emission decreases as reaction time is increased; the sample with reaction time of 1 hr has the strongest emission.

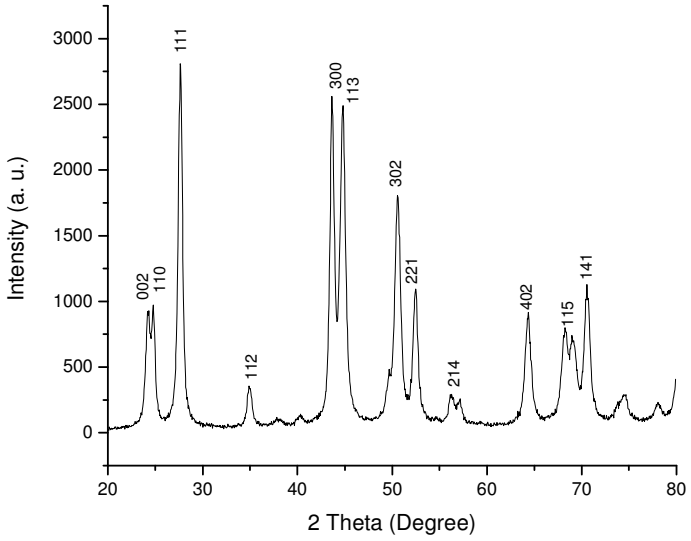

Figure 3.1 XRD pattern of $LaF_3:Ce^{3+}$ nanoparticles synthesized in water

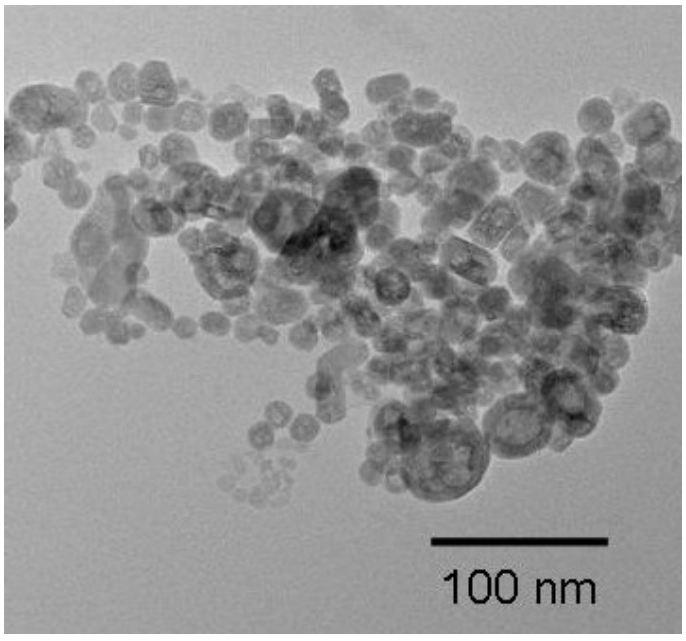

Figure 3.2 HRTEM images of $LaF_3:Ce^{3+}$ nanoparticles synthesized in water (40K)

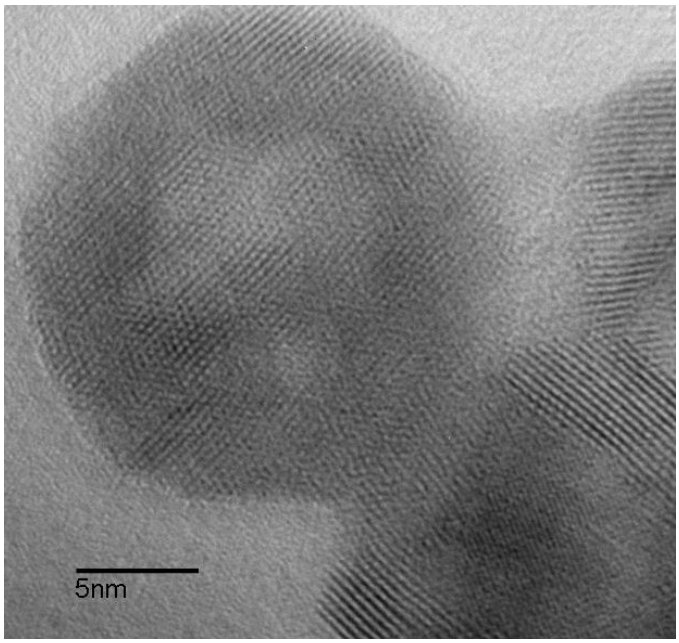

Figure 3.3 HRTEM images of $LaF_3:Ce^{3+}$ nanoparticles synthesized in water (800K)

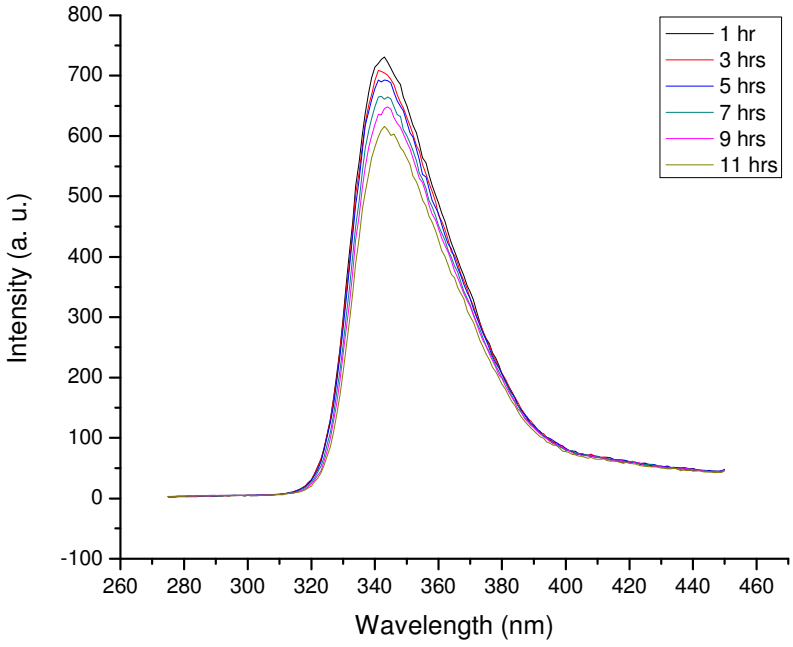

Figure 3.4 Excitation and emission spectra of LaF_3: Ce^{3+} nanoparticles at different reaction time

3.3 Luminescence Property of Water-Soluble $LaF_3:Ln^{3+}$ Nanoparticles

3.3.1 Synthesis of Water-Soluble $LaF_3:Ln^{3+}$ Nanoparticles

Lanthanum (III) nitrate hydrate ($La(NO_3)_3 \cdot X\ H_2O$, 99.9%), Cerium (III) nitrate hexahydrate($Ce(NO_3)_3\ 6H_2O$,99.9%), Terbium (III) nitrate pentahydrate($Tb(NO_3)_3 \cdot 5H_2O$, 99.9%), Ytterbium (III) nitrate pentahydrate($Yb(NO_3)_3 \cdot 5H_2O$, 99.9%), Ammonium fluoride (NH_4F, 99.9%), poly(ethylene glycol) bis(carboxymethyl) ether were purchased from Sigma-Aldrich. All of the reagents were used directly, without further purification.

$LaF_3:Tb^{3+}$ nanoparticles were synthesized using the wet-chemistry method with different dopant concentrations, $La_{0.7}Tb_{0.3}F_3$ and $La_{0.8}Tb_{0.2}F_3$ nanoparticles. Typically, the $La_{0.7}Tb_{0.3}F_3$ nanoparticle was synthesized according to the following protocol: 2.8 mmol of $La(NO_3)_3 \cdot XH_2O$, 1.2 mmol of $Tb(NO_3)_3 \cdot 5H_2O$ and 10.5 mmol of NH_4F in 10ml water solution were added to 90 ml water in a three-necked flask, 1 ml of PEG was added dropwise to the mixed chemical solution as stabilizer to prevent the particles from aggregation. The $La_{0.8}Tb_{0.2}F_3$ nanoparticle was synthesized following the same protocol as the former except that 3.2 mmol of $La(NO_3)_3 \cdot XH_2O$ and 0.8 mmol of $Tb(NO_3)_3 \cdot 5H_2O$ is used instead of 2.8 mmol of $La(NO_3)_3 \cdot XH_2O$ and 1.2 mmol of $Tb(NO_3)_3 \cdot 5H_2O$. The chemicals were mixed thoroughly with stirring for half an hour at room temperature; the mixture was subsequently heated to 100° C under vigorous magnetic stirring and nitrogen protection. A white suspension was formed gradually upon stirring. The nanoparticles obtained were collected by centrifugation, washed with DI water several times, and then easily dissolved in DI water.

$LaF_3:Yb^{3+}Tb^{3+}$ nanoparticles ($La_{0.4}Yb_{0.45}Tb_{0.15}F_3$) were synthesized as follows: 1.6 mmol of $La(NO_3)_3 \cdot XH_2O$, 0.6 mmol of $Tb(NO_3)_3 \cdot 5H_2O$, 1.8 mmol of $Yb(NO_3)_3 \cdot 5H_2O$ and 10.5 mmol of NH_4F in 10 ml of water solution were added to 90 ml of water in a three-necked flask, 1 ml of PEG was added dropwise to the mixed chemical solution as stabilizer to prevent the particles from aggregation. The chemicals were mixed thoroughly with stirring for half an hour at room

temperature; the mixture was subsequently heated to 100° C under vigorous magnetic stirring and nitrogen protection. A white suspension formed gradually upon stirring. The nanoparticles obtained were collected by centrifugation, washed with DI water several times, then easily dissolved in DI water.

$LaF_3:Ce^{3+}Tb^{3+}$ nanoparticles ($La_{0.4}Ce_{0.45}Tb_{0.15}F_3$) were prepared as follows: 1.6 mmol of $La(NO_3)_3{\cdot}XH_2O$, 0.6 mmol of $Tb(NO_3)_3 \cdot 5H_2O$, 1.8 mmol of $Ce(NO_3)_3 \cdot 6H_2O$ and 10.5 mmol of NH_4F in 10 ml water solution were added to 90 ml of water in a three-necked flask, 1 ml of PEG was added dropwise to the mixed chemical solution as stabilizer to prevent the particles from aggregation. The chemicals were mixed thoroughly with stirring for half an hour at room temperature; the mixture was subsequently heated to 100° C for 2 hours under vigorous magnetic stirring and nitrogen protection. A white cloudy solution formed homogeneously upon stirring. The nanoparticles were formed directly as water-soluble particles.

3.3.2 Characterization of Water-Soluble $LaF_3:Ln^{3+}$ Nanoparticles

The fluorescence spectra of the samples were measured using a fluorescence spectrometer (RF-5301PC) with a 400W monochromatized xenon lamp and 3/3 slit widths. Figures 3.5 and 3.6 show the excitation and emission spectra of $La_{0.7}Tb_{0.3}F_3$ and $La_{0.8}Tb_{0.2}F_3$ nanoparticles. We see that both Figure 3.5 and Figure 3.6 contain four sharp emission peaks, at 490 nm, 543 nm, 584 nm and 621 nm, although the intensity of emissions in Figure 3.5 is stronger than that in Figure 3.6. The emission peaks are generally assigned to $^5D_4 \rightarrow {}^7F_j$ (j=3-6) transitions of Tb^{3+}. We conclude that $La_{0.7}Tb_{0.3}F_3$ water-soluble nanoparticles have stronger luminescence than $La_{0.8}Tb_{0.2}F_3$ nanoparticles. Figures 3.7 and 3.8 show the excitation and emission spectra of water-soluble nanoparticles $La_{0.4}Yb_{0.45}Tb_{0.15}F_3$ and $La_{0.4}Ce_{0.45}Tb_{0.15}F_3$. The characteristic emission peaks of Tb^{3+} are observed from both nanoparticles, and clearly the emission intensity of $La_{0.4}Ce_{0.45}Tb_{0.15}F_3$ is much stronger than that of $La_{0.4}Yb_{0.45}Tb_{0.15}F_3$. The emission intensity from Ce^{3+} in $La_{0.4}Ce_{0.45}Tb_{0.15}F_3$ is very weak and there may be an energy

transfer from Ce^{3+} to Tb^{3+}. As a result, the emission of $La_{0.4}Ce_{0.45}Tb_{0.15}F_3$ is significantly stronger than that of $La_{0.4}Yb_{0.45}Tb_{0.15}F_3$. However, in the case of $La_{0.4}Yb_{0.45}Tb_{0.15}F_3$, it seems there is no energy transfer from Yb^{3+} to Tb^{3+}.

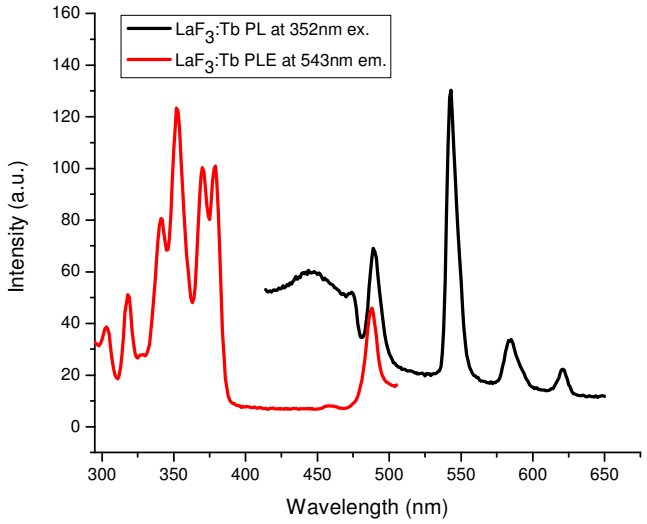

Figure 3.5 Excitation and emission spectra of LaF_3: Tb ($La_{0.7}Tb_{0.3}F_3$) nanoparticles

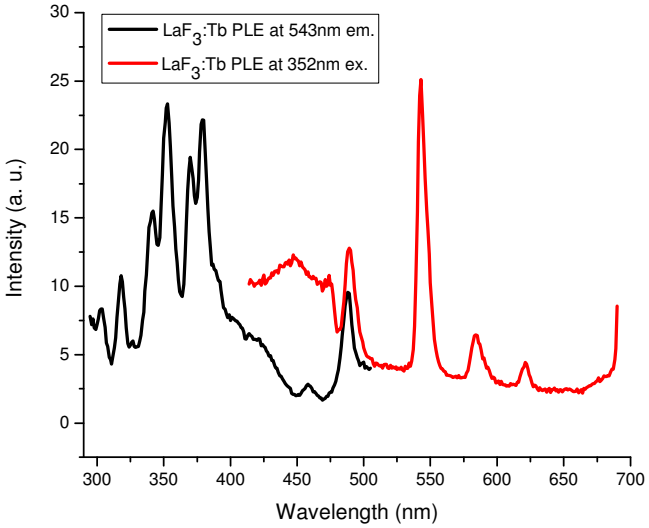

Figure 3.6 Excitation and emission spectra of LaF_3: Tb ($La_{0.8}Tb_{0.2}F_3$) nanoparticles

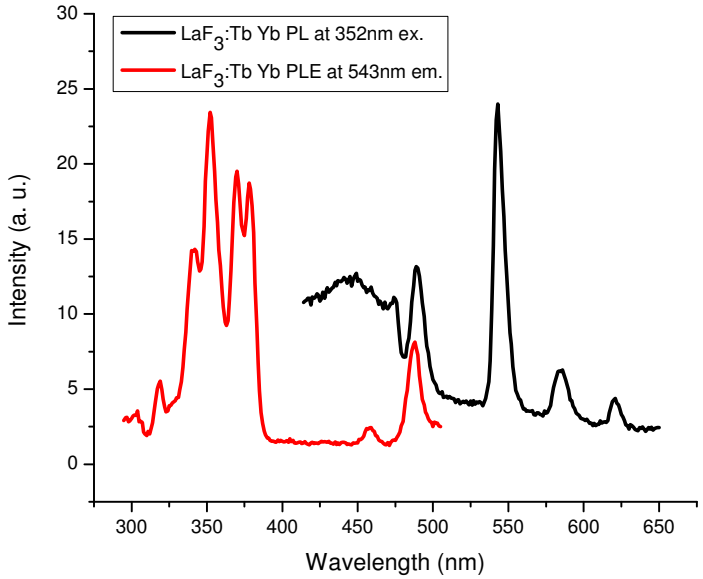

Figure 3.7 Excitation and emission spectra of LaF_3: TbYb ($La_{0.4}Yb_{0.45}Tb_{0.15}F_3$) nanoparticles

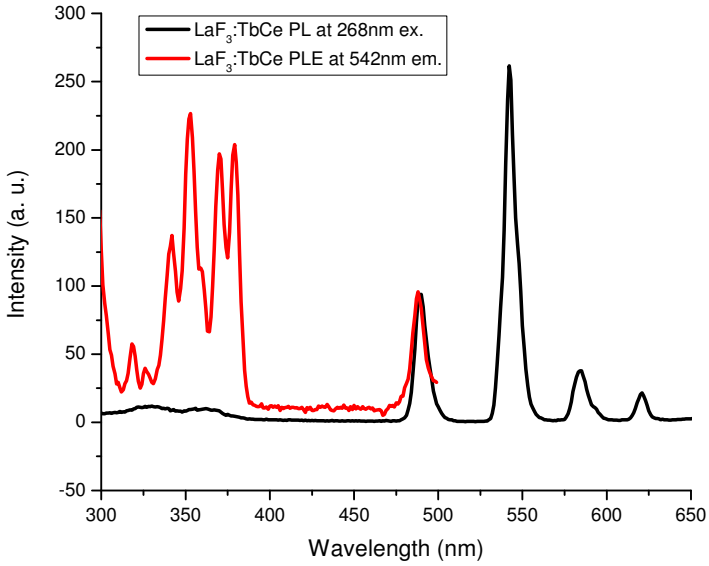

Figure 3.8 Excitation and emission spectra of LaF_3: TbCe nanoparticles

3.4 Conclusion

We synthesized Ln^{3+} doped LaF_3 nanoparticles in water using the wet-chemistry method. The X-ray diffraction (XRD) pattern shows that LaF_3:Ce was synthesized. Transmission electron microscopy (TEM) clearly shows the nanocrystal's lattice fringes. Also, the average size of these nanoparticles is about 15 nm, which is consistent with the size obtained from XRD measurement. The nanoparticles have an emission peak at 343 nm, which was attributed to the 5d→4f transitions of the Ce ion. Intensity of emission decreases as reaction time is increased; the sample with a reaction time of 1 hr has the strongest emission. Water-soluble Ln^{3+} doped LaF_3 nanoparticles are synthesized with strong emissions at 490 nm, 543 nm, 584 nm and 621 nm. These emissions are attributed to $^5D_4 \rightarrow {}^7F_j$ (j=3-6) transitions of Tb^{3+}.

CHAPTER 4

SUMMARY AND FUTURE WORK

Tunability of emission color is very important in the development of light-emitting materials and devices. Recently, fluorescent nanoparticles have inspired growing research interest because of their variability and flexibility in materials synthesis and nanoparticle preparation, and also because of their future promise in the areas of optoelectronic materials and biological systems.

In our work, we synthesized $LaF_3:Ce^{3+}$ in DMSO with strong luminescence, where emissions can be tuned from blue to red depending on temperature and reaction time. DMSO has been shown to be a carrier of drugs across membranes. It is more successful ferrying some drugs, such as morphine sulfate, penicillin, steroids, and cortisone, than others, such as insulin. This property would enable DMSO to act as a new drug delivery system that would lower the risk of infection due to penetration of the skin. By using DMSO as a solvent, the $LaF_3:Ce^{3+}$ nanoparticles we synthesized could be used in drug delivery, biological labels and in other areas. Further research in toxicity is needed.

In most biological application, especially in vivo application, nanoparticles are must be water soluble and biocompatible. However, more than 40% of compounds identified through combinatorial screening programs are poorly soluble in water. These molecules are difficult to formulate using conventional approaches and are associated with innumerable formulation-related performance issues. Formulating these compounds as pure drug nanoparticles is one of the newer drug-delivery strategies applied to this class of molecules. The formulations consist of water, drug, and one or more generally regarded as safe recipients. These liquid dispersions

exhibit an acceptable shelf-life and can be postprocessed into various types of solid dosage forms. Most commonly, nanoparticles constructed for use in vivo would be soluble in water, but the techniques available for making water-soluble nanoparticles generate particles with a wide distribution in size and often of poor quality. In our research, we have developed a simple chemical method for making high-quality, well-defined, water-soluble lanthanide doped LaF_3 nanoparticles. These nanoparticles could benefit in the application of biological labels in radiation therapy for cancer treatment.

REFERENCES

[1] Taniguchi N. On the basic concept of 'nano-technology' *Proceedings of the International Conference of Production Engineering*. Tokyo, Japan: Society of Precision Engineering; 1974.

[2] Dowling, A., Clift, R., Grobert, N., Hutton, D., Oliver, R., O'neill, O., Pethica, J., Pidgeon, N., Porritt, J., Ryan, J., Seaton, A., Tendler, S., Welland, M., Whatmore, R., 2004. Nanoscience and Nanotechnologies: Opportunities and Uncertainties. The Royal Society and the Royal Academy of Engineering, London, UK.

[3] Borm, P.J., Robbins, D., Haubold, S., Kuhlbusch, T., Fissan, H., Donaldson, K., Schins, R., Stone, V., Kreyling, W., Lademann, J., Krutmann, J., Warheit, D., Oberdorster, E., 2006b. The potential risks of nanomaterials: a reviewcarried out for ECETOC. Part. Fibre Toxicol. 3, 11.

[4] Nanoscience and nanotechnologies: opportunities and uncertainties, The Royal Society, July, **2004**.

[5] Buffat, Ph. & Burrel, J.-P., *Physical Review A* **1976**,13 (6): 2287 – 2298.

[6] Gao, X.; Cui, Y.; Levenson, R. M.; Chung, L. W.; Nie, S. *Nat. Biotechnol.* **2004**, *22*, 969–976.

[7] Tada, H.; Higuchi, H.; Wanatabe, T. M.; Ohuchi, N. *Cancer Res.* **2007**, *67*, 1138–1144.

[8] Akerman, M. E.; Chan, W. C.; Laakkonen, P.; Bhatia, S. N.; Ruoslahti, E. *Proc. Natl. Acad. Sci. U.S.A.* **2002**, *99*, 12617–12621.

[9] Montet, X.; Montet-Abou, K.; Reynolds, F.; Weissleder, R.; Josephson, L. *Neoplasia (Ann Arbor, MI, U.S.)* **2006**, *8*, 214–222.

[10] Cai, W.; Shin, D.-W.; Chen, K.; Gheysens, O.; Cao, Q.; Wang, S. X.; Gambhir, S. S.; Chen, X. *Nano Lett.* **2006**, *6*, 669–676.

[11] Michalet, X.; Pinaud, F. F.; Bentolila, L. A.; Tsay, J. M.; Doose, S.; Li, J. J.; Sundaresan, G.; Wu, A. M.; Gambhir, S. S.; Weiss, S. *Science* **2005**, *307*, 538–544.

[12] Li, Z. B.; Cai, W.; Chen, X. *J. Nanosci. Nanotechnol.* **2007**, *7*, 2567–2581.

[13] Medintz, I. L.; Uyeda, H. T.; Goldman, E. R.; Mattoussi, H. *Nat. Mater.* **2005**, *4*, 435–446.

[14] Soltesz, E. G.; Kim, S.; Laurence, R. G.; DeGrand, A. M.; Parungo, C. P.; Dor, D. M.; Cohn, L. H.; Bawendi, M. G.; Frangioni, J. V.; Mihaljevic, T. *Ann. Thoracic Surg.* **2005**, *79*, 269–277.

[15] Ballou, B.; Ernst, L. A.; Andreko, S.; Harper, T.; Fitzpatrick, J. A. J.; Waggoner, A. S.; Bruchez, M. P. *Bioconjugate Chem.* **2007**, *18*, 389–396.

[16] Knapp, D. W.; et al. *Eur. Urol.*, in press.

[17] Frangioni, J. V.; Kim, S. W.; Ohnishi, S.; Kim, S.; Bawendi, M. G. *Methods Mol. Biol.* **2007**, *374*, 147–160.

[18] Wang, C.-W.; Moffitt, M. G. *Langmuir* **2005**, *21*, 2465-2473.

[19] Ba¨umle, M.; Stamou, D.; Segura, J.-M.; Hovious, R.; Vogel, H. *Langmuir* **2004**, *20*, 3828-3831.

[20] Meziani, J. M.; Pathak, P.; Harruff, B. A.; Hurezeanu, R.; Sun, Y.-P. *Langmuir* **2005**, *21*, 2008-2011.

[21] Charvet, N.; Reiss, P.; Roget, A.; Dupuis, A.; Gru¨nwald, D.; Carayon, S.; Chandezon, F.; Livache, T. *J. Mater. Chem.* **2004**, *14*, 2638-2642.

[22] Powe, A. M.; Fletcher, K. A.; St. Luce, N. N.; Lowry, M.; Neal, S.; McCarroll, M. E.; Oldham, P. B.; McGown, L. B.; Warner, I. M. *Anal. Chem.* **2004**, *76*, 4614-4634.

[23] Sun, C.; Yang, J.; Ki, L.; Wu, X.; Liu, Y.; Liu, S. *J. Chromatogr., B* **2004**, *803*, 173-190.

[24] Alivisatos, P., Nat. Biotechnol. **2004**.22 (1), 47–52.

[25] Daniel, M.C., Astruc, D., Chem. Rev. **2004**.104, 293–346.

[26] Penn, S.G., He, L., Natan, M.J., Curr. Opin. Chem. **2003**. Biol. 7, 609–615.

[27] Shipway, A.N., Katz, E., Willner, I., Chem. Phys. Chem. **2000**. 1, 18–52.

[28] Kubitschko, S., Spinke, J., Br¨uckner, T., Pohl, S., Oranth, N., **1997**. Anal. Biochem. 253, 112–122.

[29] Kambhampati, D.K., Knoll, W., Curr. Opin. Colloid Interf. Sci. **1999**. 4, 273–280.

[30] Rich, R.L., Myszka, D.G., J. Mol. Recognit. **2000**, 13, 388–407.

[31] Schultz, S., Smith, D.R., Mock, J.J., Schultz, D.A., **2000**. PNAS 97 (3), 996–1001.

[32] Psaras P A and Langford H D (ed) **1987** Advancing Materials Research, US National Academy of Engineering and National Academy of Sciences (Washington, DC: National Academy Press) p 203

[33] LaMer V K and Dinegar R H **1950** J. Am. Chem. Soc. 72 4847 Overbeek J T G **1982** Adv. Colloid Interface Sci. 15 251 Sugimoto T **1987** Adv. Colloid Interface Sci. 28 65

[34] Nielsen F **1982** Manufact. Chemist 53 38

[35] Real M W **1986** Proc. Br. Ceram. Soc. 38 59

[36] Rosen M J (ed) **1987** Surfactants in Emerging Technologies (New York: Dekker)

[37] McHale A E **1991** Ceramics and Glasses, Engineered Materials Handbook vol 4 (Metals Park, OH: ASM) p 115

[38] R.L. Whetten, J.T.Khoury, M.M. Alvarez, S. Murthy, I. Vezmar, Z.L. Wang, P. W. Stephens, C. L. Cleveland, W. D. Luedtke, and U. Landman, Adv. Mater. **1996**, 8, 428-433

[39] C.B. Murray, C.R. kagan, and M.G. Bawendi, Science **1995**, 270, 1335-1338

[40] G. Binnig, H. Rohrer, Ch. Gerber, and E. Weibel, Phys. Rev. Lett. **1982**, 49, 57-60

[41] J.R. Power et al., Phys. Rev. Lett. **1998**, 80, 3133.

[42] Lewin, M.; Carlesso, N.; Tung, C.-H.; Tang, X.-W.; Cory, D.; Scadden, D. T.; Weissleder, R. *Nat. Biotechnol.* **2000**, *18*, 410.

[43] Lu, H.; Yi, G.; Zhao, S.; Chen, D.; Guo, L.-H.; Jing, C. *J. Mater. Chem.* **2004**, *14*, 1336.

[44] Levy, L.; Sahoo, Y.; Kim, K.-S.; Bergey, E. J.; Prasad, P. N. *Chem. Mater.* **2002**, *14*, 3715.

[45] Lal, M.; Levy, L.; Kim, K. S.; He, G. S.; Wang, X.; Min, Y. H.; Pakatchi, S.; Prasad, P. N. *Chem. Mater.* **2000**, *12*, 2632.

[46] (a) Tissue, B. M. *Chem. Mater.* **1998**, *10*, 2837. (b) Gordon, W. O.; Carter, J. A.; Tissue, B. M. *J. Lumin.* **2004**, *108*, 339.

[47] Feng, J.; Shan, G.; Maquieira, A.; Koivunen, M. E.; Guo, B.; Hammock, B. D.; Kennedy, I. M. *Anal. Chem.* **2003**, *75*, 5282.

[48] Tan, M.; Wang, G.; Hai, X.; Ye, Z.; Yuan, J. *J. Mater. Chem.* **2004**, *14*, 2896.

[49] Weber, M. J. *Phys. Re*V. **1967**, *157*, 262.

[50] Klink, S. I.; Hebbink, G. A.; Grave, L.; van Veggel, F. C. J. M.; Reinhoudt, D. N. R.; Slooff, L. H.; Polman, A.; Hofstraat, J. W. *J.Appl. Phys.* **1999**, *86*, 1181.

[51] Blasse G and Grabmaier B C 1994 *Luminescent Materials* (Berlin: Springer).

[52] Henderson B and Imbusch G F 1989 *Optical Spectroscopy in Inorganic Solids* (Oxford: Oxford University Press).

[53] Z. Ye, M. Tan, G. Wang, and J. Yuan. *J. Mater. Chem.* **2004**, 14, 851–856.

[54] X. D. Hai, M. Q. Tan, G. Wang, Z. Q. Ye, J. L. Yuan, and K. Matsumoto *Anal. Sci* **2004**, 20, 245–246.

[55] Meiser F, Cortez C and Caruso F *Angew. Chem. Int. Edn* **2004**, 43 5954–5957.

[56] Beaurepaire E *et al Nano Lett.* **2004**, 4, 2079–2083.

[57] M. J. Roberts, M. D. Bentley, and J. M. Harris *Adv. Drug Deliv. Rev.* **2002**, 54, 459–476.

[58] A. M. Derfus, W. C. W. Chan and S. N. Bhatia. *Adv. Mater*. **2004**, 12, 961–966.

[59] Herschler, R., Jacob, S.W. The case of dimethyl sulfoxide. In: Lasagna, L. (Ed.), *Controversies in Therapeutics*. Philadelphia: W.B. Saunders, 1980.

[60] Salim, A. *Oncology* **1992**, 49:58-62.

[61] Staritzky, E.; Asprey, L. B. *Analytical Chemistry* **1957**, *29*, 856.

[62] Yanes, A. C.; Del-Castillo, J.; Me´ndez-Ramos, J.; Rodrı´guez, V. D.; Torres, M. E.; Arbiol, J. *Optical Materials* **2007**, *29*, 999.

[63] Y. Zorenko, T. Voznyak, V. Vistovsky el. Radiation Measurements 2007, 42, 648-651.

[64] P. Rodnyi, E. Melchakov, N. Zakharov, I. Munro, A. Hopkirk , Journal of Luminescene **1995**, 65, 85-89.

[65] Lu HC, Yi GS, Zhao SY, Chen DP, Guo LH, Cheng J J Mater Chem **2004**, 14:1336–1341.

[66] Stouwdam JW, van Veggel FCJM Nano Lett. **2002**, 2:733–737.

[67] Diamente PR, Burke RD, van Veggel FCJM Langmuir **2006**, 22:1782–1788.

[68] G. Franzo, F. Iacona, V. Vinciguerra, F. Priolo, Mater. Sci. Eng. B: Solid 69 **2000**, 335.

[69] W.L. Fan,W. Zhao, L.P. You, X.Y. Song,W.M. Zhang, H.Y. Yu, S.X. Sun, J. Solid State Chem. **2004**, 177, 4399.

[70] M. Haase, K. Riwotzki, H. Meyssamy, J. Alloys Compd. **2000**, 303, 191.

[71] D. Marrero-Lopez, P. Nunez, M. Abril, J. Non-Cryst. Solids **2004**, 345, 377.

[72] Y.B. Xie, C.W. Yuan, Mater. Res. Bull. **2004**,39, 533.

[73] L.M. Chen, Y.N. Liu, Y.D. Li, J. Alloys Compd. **2004**, 381, 266.

[74] H.W. Song, L.X.Yu, L.M.Yang, S.Z. Lu, J. Nanosci. Nanotechnol. **2005**, 5, 1519.

BIOGRAPHICAL INFORMATION

The author received her Master degree in condensed matter physics from Tongji University in China in March 2002; she received another Master degree in Bio-nano physics from University of Texas at Arlington in August 2008. She will continue studying for her Ph. D.